Journal of Inorganic Biochemistry 150 (2015) 9–17

Contents lists available at ScienceDirect

Journal of Inorganic Biochemistry

journal homepage: www.elsevier.com/locate/jinorgbio

A versatile salicyl hydrazonic ligand and its metal complexes as antiviral agents

D. Rogolino [a,*], M. Carcelli [a], A. Bacchi [a], C. Compari [b], Laura Contardi [b], E. Fisicaro [b], A. Gatti [a], M. Sechi [c], A. Stevaert [d], L. Naesens [d]

[a] Dipartimento di Chimica, Parco Area delle Scienze 17/A, 43124 Parma, Italy
[b] Dipartimento di Farmacia Università di Parma, Parco Area delle Scienze 17/A, 43124 Parma, Italy
[c] Dipartimento di Chimica e Farmacia, Università di Sassari, Via Vienna 2, I-07100 Sassari, Italy
[d] Rega Institute for Medical Research, KU Leuven — University of Leuven, B-3000 Leuven, Belgium

ARTICLE INFO

Article history:
Received 9 March 2015
Received in revised form 21 May 2015
Accepted 24 May 2015
Available online 27 May 2015

Keywords:
Acylhydrazones
Chelating ligand
Metal complexes
Antiviral activity

ABSTRACT

Acylhydrazones are very versatile ligands and their coordination properties can be easily tuned, giving rise to metal complexes with different nuclearities. In the last few years, we have been looking for new pharmacophores able to coordinate simultaneously two metal ions, because many enzymes have two metal ions in the active site and their coordination can be a successful strategy to inhibit the activity of the metalloenzyme. As a part of this ongoing research, we synthesized the acylhydrazone H_2L and its complexes with Mg(II), Mn(II), Co(II), Ni(II), Cu(II) and Zn(II). Their characterization, both in solution – also by means of potentiometric studies – and in the solid state, evidenced the ability of the *o*-vanillin hydrazone scaffold to give rise to different types of metal complexes, depending on the metal and the reaction conditions. Furthermore, we evaluated both the free ligand and its metal complexes in in vitro studies against a panel of diverse DNA- and RNA-viruses. In particular, the Mg(II), Mn(II), Ni(II) and Zn(II) complexes had EC_{50} values in the low micromolar range, with a pronounced activity against vaccinia virus.

1. Introduction

Acylhydrazone-based ligands and their transition metal complexes are widely studied in catalysis [1], as building blocks in supramolecular chemistry [2,3], as anticancer agents [4,5], and, particularly interesting for our research, antiviral molecules [6,7]. They are often used to build multinuclear metal complexes since they are versatile ligands and their coordination properties can be easily tuned from an electronic and a steric point of view [8–10]. Acylhydrazone ligands, in fact, can act as bidentate or tridentate chelating ligands and even as tetradentates, and can coordinate one or more metal centers [1,3,10,11]. Complexes of salicylaldehyde hydrazones with Mn(II), Cu(II), lanthanide(III), Pd(II), and Ni(II) have been previously studied [1–3,8–11] and they represent a challenging topic from the coordination point of view. These ligands typically coordinate to the metal ion through the phenolic and carbonyl oxygens and the imine nitrogen atom. Their degree of deprotonation depends on the reaction conditions and the metal employed and they can give rise to monometallic, bis-chelated complexes or to multimetallic assemblies held together by intermolecular forces [2,3,12].

In this context, we synthesized an acylhydrazone ligand (H_2L) (Fig. 1) by condensation of *o*-vanillin with salicyl hydrazide. H_2L is diprotic and a potentially *ONOO* tetradentate ligand; it can coordinate one but also two metal ions (Fig. 1).

Its coordination compounds with Mg(II), Mn(II), Co(II), Ni(II), Cu(II) and Zn(II) were isolated and characterized by IR, elemental analysis and mass spectrometry (complexes **1**–**6**, Fig. 2); the X-ray crystal structures of the tetranuclear copper complex $\mathbf{Cu_4L_4 \cdot 4CH_3CN}$ and of the bis-chelated cobalt(III) complex $\mathbf{[CoL_2]NHEt_3}$ (**3**) are also discussed. Moreover, the solution behavior of H_2L towards Mg(II), Mn(II), Ni(II), Cu(II) and Zn(II) was investigated by means of potentiometric experiments.

It is well known that the metal complexes of hydrazones have diverse biological and pharmaceutical properties: in fact, they were studied as antimicrobial, anti-inflammatory, antifungal, anti-tubercular, anticancer, antimalarial and antiviral agents [13–16]. In the last few years, the research of new metal-chelating pharmacophores with antiviral activity is at the center of our interest [17–20]. Many enzymes

* Corresponding author at: Dipartimento Chimica, Università di Parma Campus Universitario — Parco Area delle Scienze 17/A, 43124 Parma, Italy.
E-mail address: dominga.rogolino@unipr.it (D. Rogolino).

http://dx.doi.org/10.1016/j.jinorgbio.2015.05.013
0162-0134/

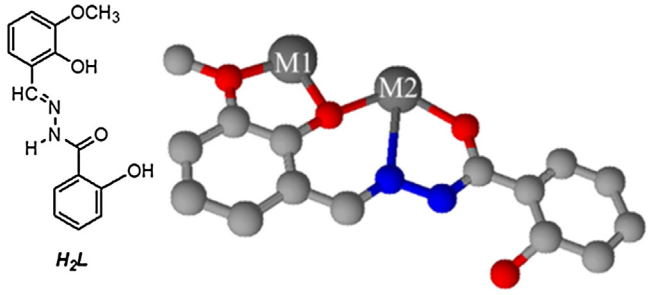

Fig. 1. Chemical structure of the acylhydrazonic ligand H_2L (left); the polydentate ligand H_2L can coordinate one or two metal ions (right).

have two metal ions in their active site and coordination of these cofactors can be a successful strategy to inhibit the activity of a given metalloenzyme [21,22]. As a part of this ongoing research, we evaluated H_2L and its metal complexes **1**–**6** in in vitro studies against a panel of diverse DNA- and RNA-viruses, discovering promising activity of this scaffold against herpes simplex virus (HSV) and vaccinia virus (VV).

2. Experimental

2.1. Material and methods

All reagents of commercial quality were used without further purification. Purity of compounds was determined by elemental analysis and verified to be ≥96% for all synthesized molecules. NMR spectra were recorded at 25 °C on a Bruker Avance 400 FT spectrophotometer. The ATR-IR spectra were recorded by means of a Nicolet-Nexus (Thermo Fisher) spectrophotometer by using a diamond crystal plate in the range of 4000–400 cm^{-1}. Elemental analyses were performed by using a FlashEA 1112 series CHNS/O analyzer (Thermo Fisher) with gas-chromatographic separation. Electrospray Ionization mass spectral analyses (ESI-MS) were performed with an ESI-TOF (electrospray ionization time-of-flight) Micromass 4LCZ spectrometer. MS spectra were acquired in positive EI mode by means of a DEP-probe (Direct Exposure Probe) mounting on the tip a Re-filament with a DSQII Thermo Fisher apparatus, equipped with a single quadrupole analyzer.

2.2. Synthesis

2.2.1. N'-(2-hydroxy-3-methoxybenzylidene)-2-hydroxybenzoylhydrazone (H_2L)

H_2L was obtained by slight modifications of reported procedures [23]. Briefly, an equimolar amount of salicyl hydrazide and aldehyde are dissolved in absolute ethanol. The mixture was refluxed for 6 h, cooled at room temperature and concentrated in vacuum. The resulting precipitate was filtered off, washed with cold ethanol and dried in vacuum. Yield = 89%. ^{1}H-NMR (DMSO-d_6, 25 °C), δ: 3.82 (s, 3H, OCH_3), 6.85–7.06 (m, 4H, ArH), 7.17 (d, J = 7.5 Hz, 1H, ArH), 7.45 (t, J = 7.6 Hz, 1H; ArH), 7.89 (d, 2H; J = 7.5, ArH), 8.69 (s, 1H; HC = N), 10.87 (s, br, 1H; NH), 11.99 (s, br, 2H; OH). ^{1}H-NMR (MeOD-d_4, 25 °C), δ: 3.91 (s, 3H, OCH_3), 6.90 (t, J = 7.6 Hz, 1H, ArH); 6.96–7.00 (m, 2H, ArH), 7.06 (d, J = 8.2 Hz, 1H, ArH), 7.21 (d, J = 8.2 Hz, 1H; ArH), 7.47 (t, 2H; J = 7.4, ArH), 7.92 (d, 2H; J = 7.7, ArH), 8.60 (s, 1H; HC = N). ^{13}C-NMR (MeOD-d_4, 25 °C), δ: 55.27; 113.79; 114.78; 117.10; 118.63; 119.01; 119.06; 121.25; 128.08; 134.02; 148.11; 149.48; 159.73. MS (EI, 70 eV) m/z (%) = 286.0 ($[M]^+$, 100);. IR (cm^{-1}): ν_{NH+OH} = 3202 (br); $\nu_{C=O}$ = 1606; $\nu_{C=N}$ = 1560; ν_{OCH3} = 1256, 1079. Anal. Calcd. for $C_{15}H_{14}N_2O_4 \cdot 1/2H_2O$: C 61.01; H 5.12; N 9.49. Found: C 61.20, H 4.89, N 9.58.

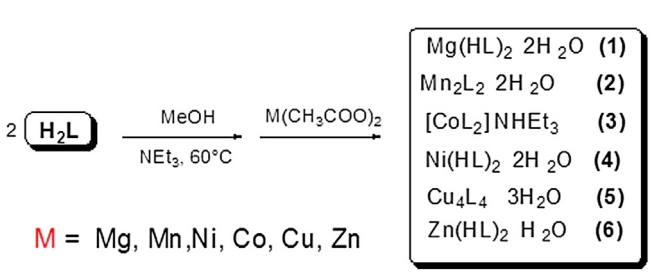

Fig. 2. Synthesis of complexes **1**–**6**.

Synthesis of the complexes **1**–**6**, general procedure. The ligand H_2L (0.5 mmol) was dissolved in 30 ml of methanol and 1 eq. of NEt_3 was added. The yellow solution was stirred at 65 °C for 30 min. 0.5 eq. of acetate of the metal were added and then the reaction mixture was stirred at reflux for 4 h, concentrated in vacuum and cooled overnight. The precipitate was filtered off, washed with water and dried under vacuum.

2.2.2. $Mg(HL)_2 \cdot 2H_2O$ (**1**)

Light yellow powder. Yield: 70%. ^{1}H-NMR (MeOD, 25 °C), δ: 3.91 (s, 3H, OCH_3); 6.88–7.07 (m, 4H, ArH); 7.20 (d, J = 7.4 Hz, 1H, ArH); 7.46 (t, J = 7.9 Hz, 1H); 7.92 (d, J = 7.9 Hz, 1H); 8.60 (s, 1H; HC = N). MS-ESI, m/z (%) = 595 ($[Mg(HL)_2 + H]^+$, 40). IR (cm^{-1}): ν_{NH} = 3267 (br); $\nu_{C=O}$ = 1627, 1609; ν_{OCH3} = 1211, 1082. Anal. Calcd. for $C_{30}H_{26}N_4O_8Mg \cdot 2H_2O$: C 57.11, H 4.79, N 8.88. Found: C 57.33, H 4.33, N 9.00.

2.2.3. $Mg_2L_2 \cdot 4H_2O$ (**1a**)

0.5 mmol of H_2L was dissolved in 30 ml of methanol and 2.5 eq. of NaOH 4 M were added. The yellow solution was stirred at 65 °C for 30 min. 1 eq. of magnesium acetate was added and the reaction mixture was stirred at reflux for 4 h, concentrated in vacuum and cooled overnight. The precipitate was filtered off and washed with water. Intense yellow powder. Yield: 64%. ^{1}H-NMR (MeOD, 25 °C), δ: 3.84 (s, br, 3H, OCH_3); 6.45 (s, br, 1H, ArH), 6.68–6.82 (m, br, 5H, ArH); 7.20 (s, br, 1H, ArH); 7.90 (s, br, 1H); 8.24 (s, br, 1H; HC═N). MS-ESI, m/z (%) = 309 ($[MgL]^+$, 100); 617 ($[Mg_2L_2]^+$, 50); 640 ($[Mg_2L_2 + Na]^+$, 40). IR (cm^{-1}): ν_{OH} = 3420–3500 (br); $\nu_{C=O}$ = 1609; ν_{OCH3} = 1211, 1082. Anal. Calcd. for $C_{30}H_{24}N_4O_8Mg_2 \cdot 4H_2O$: C 52.28, H 4.68, N 8.13. Found: C 52.67, H 4.63, N 8.03.

2.2.4. $Mn_2L_2 \cdot 2H_2O$ (**2**)

Brown powder. Yield: 70%. MS-ESI, m/z (−, %) = 624 ($[Mn(HL)_2]^-$, 95); 677 ($[Mn_2L_2]^-$, 100). IR (cm^{-1}): ν_{NH} = 3267 (br); $\nu_{C=O}$ = 1607; ν_{OCH3} = 1208. Anal. Calcd. for $C_{30}H_{24}N_4O_8Mn_2 \cdot 2H_2O$: C 50.43, H 3.95, N 7.84. Found: C 50.68, H 4.27, N 7.87.

2.2.5. $[CoL_2](NHEt_3)$ (**3**)

Brown powder. Yield: 64%. ^{1}H-NMR (DMSO-d_6, 25 °C), δ: 0.99 (t, 9H, CH_3, NEt_3), 2.50 (overlapping with solvent signal, CH_2, NEt_3), 3.36 (s, 3H, OCH_3), 6.41 (t, 1H; J = 7.6, ArH), 6.51 (d, 1H; J = 7.7, ArH), 6.67 (t, 1H, J = 8, ArH), 7.22 (m, 2H, ArH), 7.47 (d, 1H, J = 7.9, ArH),7.70 (d, 1H, J = 8, ArH), 8.93 (s, 1H; HC = N), 12.64 (s, 1H, $NHEt_3$). MS-ESI, m/z (−, %) = 627 ($[CoL_2]^-$, 100). IR (cm^{-1}): ν_{NH} = 3206 (br); $\nu_{C=O}$ = 1624; $\nu_{C=N}$ = 1598. Anal. Calcd. for $C_{36}H_{40}N_5O_8Co$: C 59.26, H 5.53, N 9.60. Found: C 59.55, H 5.48, N 9.41. Crystals suitable for X-ray diffraction analysis were obtained by slow evaporation of a methanol solution of the complex.

2.2.6. $Ni(HL)_2 \cdot 2H_2O$ (**4**)

Green powder. Yield: 87%. MS-ESI, m/z (+,%) = 629 ($[Ni(HL)_2]^+$, 70); 652 ($[Ni(HL)_2 + Na]^+$, 50). IR (cm^{-1}): ν_{NH+OH} = 3150–3200 (br); $\nu_{C=O}$ = 1629; ν_{OCH3} = 1201. Anal. Calcd. for $C_{30}H_{26}N_4O_8Ni \cdot 2H_2O$: C 54.16, H 4.55, N 8.42. Found: C 54.51, H 4.84, N 8.34.

*2.2.7. $Cu_4L_4 \cdot 3H_2O$ (**5**)*

Green powder. Yield: 46%. MS-ESI, m/z (+,%) = 348 ($[CuL]^+$, 100); 717 ($[Cu_2L_2 + Na]^+$, 40); 1392 ($[Cu_4L_4 + H]^+$, 10). IR (cm^{-1}): ν_{NH+OH} = 3150–3200 (br); $\nu_{C=O}$ = 1629; ν_{OCH3} = 1201. Anal. Calcd. for $C_{60}H_{48}N_8O_{16}Cu_4$ $3H_2O$: C 49.86, H 3.77, N 7.75. Found: C 50.00, H 3.42, N 7.60. Crystals of **$Cu_4L_4 \cdot 4CH_3CN$** suitable for X-ray diffraction analysis were obtained by recrystallization of (**5**) from acetonitrile.

*2.2.8. $Zn(HL)_2 \cdot H_2O$ (**6**)*

Yellow powder. Yield: 86%. MS-ESI, m/z (−,%) = 635 ($[Zn(HL)_2]^-$, 65). IR (cm^{-1}): ν_{NH} = 3170 (br); $\nu_{C=O}$ = 1611; $\nu_{C=N}$ = 1534. Anal. Calcd. for $C_{30}H_{26}N_4O_8Zn \cdot H_2O$: C 55.10, H 4.32, N 8.57. Found: C 55.10, H 4.00, N 8.52.

2.3. Potentiometric studies

The metal stock solutions were prepared from $MgCl_2 \cdot 6H_2O$ (Aldrich), $MnCl_2 \cdot 4H_2O$ (Janssen), $CuCl_2 \cdot 2H_2O$ (Merck), $ZnCl_2$ (Analyticals Carlo Erba) and $NiCl_2 \cdot 6H_2O$ (Merck). Their concentrations were determined by using EDTA as a titrant. Mn(II), Mg(II) and Zn(II), were titrated at pH 10 (ammonia/ammonium chloride as buffer; indicator: sodium salt of Eriochrome Black T). Mn(II) was titrated in the presence of triethanolamine and hydroxylamine chloride. For Ni(II), murexide in potassium nitrate was used as an indicator. For Cu(II), the titrations were performed in the presence of concentrated ammonia using Fast Sulfon Black as indicator. Equilibrium constants at 25 ± 0.1 °C for protonation and complexation reactions were determined by means of potentiometric measurements in methanol/water = 9:1 v/v solution at ionic strength 0.1 M KCl, carried out under nitrogen in the pH range 2.5–11. Potentiometric titrations were carried out by a fully automated apparatus equipped with a CRISON GLP 21–22 digital voltmeter (resolution, 0.1 mV) and a 5 mL Metrohm Dosimat 655 autoburet, both controlled by a homemade software in BASIC, working on an IBM computer. Temperature was controlled to ±0.1 °C by using a thermostatic circulating water bath (ISCO GTR 2000 II×). Appropriate aliquots of ligand H_2L solution, prepared by weight, were titrated with standard KOH (methanol/water = 9:1 v/v, I = 0.1 M KCl) with and without metal ions, applying constant speed magnetic stirring. Freshly boiled methanol and double-distilled water, kept under nitrogen, were used throughout. The experimental procedure to reach high accuracy in the determination of the equilibrium constants in this mixed solvent has been described in detail elsewhere [24]. The protonation constants of H_2L were obtained by titrating 20 mL of samples of the ligand (5×10^{-3} M). The speciation was defined by performing the titrations at different ligand/metal ratios (1 up to 4) and using a halved concentration of the ligand, to avoid solubility problems. At least two measurements (about 60 experimental points each) were performed for each system. The electrodic chain (Crison 5250 glass electrode and 0.1 M KCl in methanol/water = 9/1 v/v calomel electrode, Radiometer 401) was calibrated in terms of $[H^+]$ by means of a strong acid–strong base titration by Gran's method [25] allowing the determination of the standard potential, $E°$ (371.5 ± 0.4 mV), and of the ionic product of water, K_w (pK_w = 14.40 ± 0.05) in the experimental conditions used. The software HYPERQUAD [26] was used to obtain the speciation and the logarithm of the stability constants ($\log \beta_{pqr}$) from titration data. $\beta_{pqr} = [M_pL_qH_r]/[M]^p\,[L]^q\,[H]^r$ is the equilibrium constant for the reaction $pM + qL + rH = M_pL_qH_r$, in which M indicates the metal, L the completely deprotonated ligand and H the proton. Charges are omitted for simplicity.

2.4. X-ray diffractometry

Single crystals of (**3**) and of **$Cu_4L_4 \cdot 4CH_3CN$** were selected and mounted on glass fibers to collect data on a SMART Breeze diffractometer. The crystals were kept at 293 K during data collection. Table 1 reports crystal data and structure analysis. Using Olex2 [27], the structure was solved with the SIR2004 [28] structure solution program using Direct Methods and refined with the ShelXL refinement package [29] using Least Squares minimization. Anisotropic displacement parameters were refined for all non-hydrogen atoms. Hydrogen atoms were partly introduced in calculated positions riding on their carrier atoms. Compound (**3**) was seriously twinned, as shown by the high final R factors and by the high residuals in the final difference Fourier map, located close to the metal atom. Nevertheless, the structure gave useful information about the connectivity and packing organization. Hydrogen bonds were analyzed with PARST97 [30] and the Cambridge Structural Database software [31,32] was used for the analysis of the crystal packing. Crystallographic data for (**3**) and **$Cu_4L_4 \cdot 4CH_3CN$** have been deposited with the Cambridge Crystallographic Data Centre as supplementary publication no. CCDC 1050872 and CCDC 1050873. Copies of the data can be obtained free of charge on application to CCDC, 12 Union Road, Cambridge CB2 1EZ, UK (fax: (+44) 1223-336-033; e-mail: deposit@ccdc.cam.ac.uk).

Table 1
Crystal data and structure refinement for (**3**) and **$Cu_4L_4 \cdot 4CH_3CN$**.

	$Cu_4L_4 \cdot 4CH_3CN$	3
Empirical formula	$(C_{15}H_{12}CuN_2O_4)_4 \cdot 4CH_3CN$	$C_{36}H_{40}CoN_5O_8$
Formula weight	1555.44	729.66
Temperature/K	293(2)	293(2)
Crystal system	Tetragonal	Monoclinic
Space group	$I4_1/a$	$P2_1/n$
a/Å	13.470(1)	10.375(2)
b/Å	13.470	17.306(3)
c/Å	38.680(4)	19.457(3)
α/°	90	90
β/°	90	106.201(3)
γ/°	90	90
Volume/Å^3	7018.6(16)	3355(1)
Z	16	4
ρ_{calc} g/cm^3	1.472	1.445
μ/mm^{-1}	1.271	0.573
F(000)	3184.0	1528.0
Radiation	MoKα (λ = 0.71073)	MoKα (λ = 0.71073)
2Θ range/°	3.202 to 48.052	3.208 to 49.65
Reflections collected	34,451	13,784
Independent reflections	2760	13,784
Data/restraints/parameters	2760/0/231	13,784/0/458
Goodness-of-fit on F^2	1.024	1.120
Final R indexes [I ≥ 2σ (I)]	R_1 = 0.0379	R_1 = 0.1484
	wR_2 = 0.0844	wR_2 = 0.3472
Final R indexes [all data]	R_1 = 0.0678,	R_1 = 0.1881,
	wR_2 = 0.0965	wR_2 = 0.3853
Largest ΔF max/min/e Å^{-3}	0.34/−0.21	3.75/−1.09

2.5. Biological studies

The compounds' antiviral activity in cell culture was determined by cytopathic effect (CPE) reduction assays with a broad and diverse panel of viruses. The following viruses were investigated on human embryonic lung fibroblast cells: herpes simplex virus type 1 (HSV-1) strain KOS; a thymidine kinase-deficient (TK^-) HSV-1 KOS strain resistant to acyclovir; herpes simplex virus type 2 (HSV-2) strain G; vaccinia virus (Lederle strain); a clinical isolate of human adenovirus type 2 (Ad2); and vesicular stomatitis virus (VSV). The viruses assessed on human cervix carcinoma HeLa cells were: VSV; Coxsackie B4 virus; and respiratory syncytial virus (RSV). African Green Monkey Vero cells were used to study the antiviral effect on para-influenza-3 virus; reovirus-1; Sindbis virus; Coxsackie B4 virus and Punta Toro virus. Human influenza A/H1N1, A/H3N2 and B viruses were examined on Madin–Darby canine kidney (MDCK) cells. Finally, the activity against human immunodeficiency virus type 1 and type 2 (HIV-1 and HIV-2) was assessed in human MT-4 lymphoblast cells.

Semiconfluent cell cultures in 96-well plates were inoculated with the virus at a multiplicity of infection of 100 $CCID_{50}$ (50% cell culture

infective dose) or 20 PFU (plaque forming units) per well. Simultaneously with the virus, serial dilutions of the test or reference compounds were added. The plates were incubated at 37 °C (or 35 °C in the case of influenza virus) until clear CPE was reached, i.e., during 3 to 6 days, except for Ad2 which required 10 days incubation. Microscopic scoring was then performed to determine the antiviral activity [expressed as 50% effective concentration (EC_{50})] and cytotoxicity [expressed as minimum cytotoxic concentration (MCC)]. In the case of HIV-1 and HIV-2, virus-induced CPE was determined by a colorimetric formazan-based cell viability assay.

3. Results and discussion

3.1. Chemistry

The ligand H_2L (Fig. 1) was easily prepared in high yields by condensation of salicyl hydrazide and *o*-vanillin [23] and it was satisfactorily characterized. It is present in the *E* form in solution, as evidenced by the chemical shift values of the HC═N and NH proton in the ^{1}H-NMR spectrum registered in DMSO-d_6 [33]. The ligand can behave as bi-, tri- or tetradentate; in fact, there are diverse O and N donor atoms in suitable positions to coordinate one or several metal centers. To explore its coordination possibilities, H_2L was reacted with the acetates of some divalent metal ions (Mg, Mn, Co, Ni, Cu and Zn) in the presence of a base (NEt_3), yielding the corresponding metal complexes **1**–**6** (Fig. 2). Both the 1:1 and the 1:2 metal to ligand ratio were used, but in all cases, in the presence of one equivalent of base the same chemical species (i.e., complexes **1**–**6**, Fig. 2) were recovered. The IR spectra of the complexes were analyzed in comparison with that of H_2L. In the IR spectra of the magnesium, nickel and zinc complexes (**1**, **4** and **6**) the absorptions associated with the NH group (2993–3211 cm^{-1} in the ligand) are still present, which indicates that NH is not deprotonated upon complexation. In the manganese, cobalt and copper complexes (**2**), (**3**) and (**5**), instead, the NH absorption band is absent, and the ligand results bideprotonated (OH and NH). It is more difficult to rationalize the behavior of the C═O absorption. This is a strong band around 1605 cm^{-1} in H_2L; it is not significantly shifted in (**2**) and (**6**), while there is an upper shift of about 20 cm^{-1} in the other metal complexes. On the contrary, the C═O band in acylhydrazones usually undergoes a downshift upon complexation [34–36]. It has to be taken into account that in H_2L the C═O group is probably involved in an intramolecular hydrogen bond, as observed in the crystal structure of analogous molecules [37,38], and this results in an abnormally lower IR value ($\nu_{C=O}$ = 1605 cm^{-1} in H_2L and about 1650 cm^{-1}, generally, in acylhydrazones) [34–36]. The shift of the band due to coordination to the metal ion could be comparable to the lowering induced by intramolecular hydrogen interaction (about 30–50 cm^{-1}). Therefore, it is reasonable to consider that in (**2**) and (**6**) the carbonyl oxygen is coordinated to the metal. X-ray diffraction analysis has confirmed this hypothesis also for (**3**) and (**5**), where the ligand effectively coordinates the metal in the keto form.

For (**1**), (**4**) and (**6**), it is possible to suggest the formation of a bis-chelated compound $M(HL)_2$, where the ligand is monodeprotonated and coordinates to the metal by means of the phenolic oxygen, the iminic nitrogen and the carbonylic oxygen. For complex (**2**), instead, a dinuclear metal complex of type Mn_2L_2 was isolated. ESI-MS and elemental analysis support such hypothesis. The potentiometric measurements discussed in the following section indicate for magnesium the presence of another species in solution with a Mg:ligand 1:1 ratio. To isolate this species, magnesium acetate was allowed to react with H_2L in the presence of 2.5 equivalents of NaOH (pH 8–9) in a 1:1 metal to ligand ratio: in these conditions, the new complex (**1a**) was effectively isolated. In (**1a**) the ligand is bideprotonated (in the IR spectrum, the band associated to the NH absorption at 3267 cm^{-1}, which is clearly visible in the spectrum of (**1**), is absent). On the basis of the ESI-MS spectrum and some examples in the literature [3], the formation of a dinuclear Mg_2L_2 structure is proposed (Fig. 3).

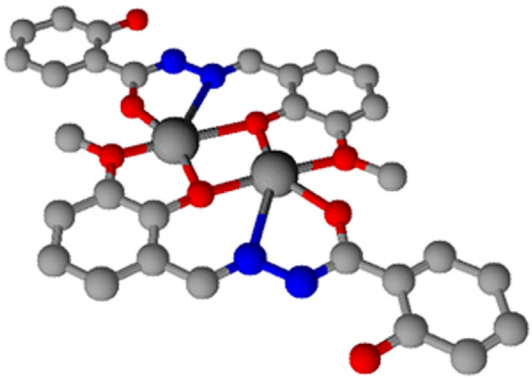

Fig. 3. Proposed coordinating mode of H_2L in the complexes (**1a**) and (**2**).

In the ^{1}H-NMR spectrum in d_6-DMSO of **1** and **1a** there are two sets of signals: one attributable to the free ligand, and one to the magnesium(II) complex. The use of a coordinating solvent, therefore, causes partial decoordination of the ligand. On the contrary, in the spectra of (**1**) and (**1a**) in MeOD there is a unique set of signals. In the ^{1}H-NMR spectrum of (**1**), the signals are sharp, with only a 0.01–0.02 ppm shift vs the free ligand; in the spectrum of (**1a**), instead, the signals are very broad and the chemical shifts are slightly different. In particular, the aromatic proton in *ortho* to the methoxy group and the methoxy protons themselves are shifted downfield of 0.4 and 0.07 ppm respectively, thus the involvement of the methoxy moiety in coordination is probable (Fig. 3).

ESI-MS data and solution studies (see below) suggest that also the manganese complex (**2**) is a dinuclear species Mn_2L_2, with the ligand bideprotonated (Fig. 3). In the literature there are some examples of dinuclear and multinuclear clusters of manganese with 2-hydroxy-3-methoxy-benzoylhydrazone [12] or 2-hydroxy-3-methoxy-benzylidene acetohydrazide [3] and, even when a mononuclear stoichiometry is isolated at the solid state, multinuclear systems are proposed in solution [11].

Some examples are present in the literature of cobalt complexes with acylhydrazonic ligands, with formation of mononuclear and polynuclear metal complexes [39–41]. During the synthesis in the presence of NEt_3, Co(II) is oxidized to Co(III) and the ionic complex **$[CoL_2](NHEt_3)$** (**3**) was isolated. The presence of a diamagnetic compound was confirmed by the registration of the ^{1}H-NMR spectrum in d_6-DMSO, where it is possible to observe the signals of the triethylammonium counterion and the bideprotonated ligand. Compared to H_2L, the aromatic protons have a shift to higher fields of about 0.3–0.4 ppm and to lower fields of about 0.35 ppm for the iminic proton. In the MS-ESI(−) spectrum there is the signal relative to the $[CoL_2]^-$ species. Diffraction analysis on a single crystal of **3** confirmed definitively the formation of a bis-chelated ionic compound (see below).

As also recently reported in the literature, acylhydrazones could be suitable ligands for the synthesis of multinuclear copper complexes [8,42]. The reaction of copper(II) acetate with H_2L afforded the green tetranuclear complex **$Cu_4L_4 \cdot 3H_2O$** (**5**); crystals of **$Cu_4L_4 \cdot 4CH_3CN$** were obtained by recrystallization of (**5**) from acetonitrile and characterized by X-ray diffraction analysis. It is interesting to note that the presence of the Cu_4L_4 species was confirmed in solution by means of ESI-MS (see Supplementary material). In (**5**) the ligand is bideprotonated, as inferred also by IR data, and coordinates to the metal in an ONO fashion, through the deprotonated phenolic oxygen, the iminic nitrogen and the carbonylic oxygen. It is well known [43–47] that acylhydrazones exhibit keto–enol tautomerism in solution and that, if complexation is followed by deprotonation of the ligand, the enol form is stabilized. In the case of (**5**), instead, the ligand coordinates to the metal center in the keto form (see crystal structure analysis and $\nu_{C=O}$ = 1629 cm^{-1}).

3.2. X-ray analysis

Compound **$Cu_4L_4 \cdot 4CH_3CN$** is obtained by crystallization from acetonitrile, that is found in the packing of the crystal structure together with the tetranuclear complex. **$Cu_4L_4 \cdot 4CH_3CN$** crystallizes in the tetragonal space group $I4_1/a$, and the molecular structure of the complex is shown in Figs. 4 and 5.

The Cu_4L_4 neutral molecule is based on the monomeric unit shown in Fig. 4, built by the coordination of the bideprotonated ligand to one copper(II) ion, in a tridentate O—N—O chelation that generates one five-membered and one six-membered chelation ring with bite angles of 82(1)° and 93(1)°, respectively. The unit is practically planar (rms deviation from planarity = 0.18 Å), since the rotatable terminal 2-hydroxy-phenyl ring is locked in the plane by an intramolecular hydrogen bond to the amidic nitrogen [O4—H…N1 = 2.593(6) Å, 128(6)°]. This intramolecular hydrogen bond in acylhydrazonic ligands similar to H_2L has been observed in analogous coordination compounds, and, interestingly, it points to the stabilization of the keto form in the keto-enol tautomerism of the ligand [48]. The tetranuclear neutral complex (Fig. 5) is generated by a fourfold rotoinversion axis whereby the hydrazonic carbonyl O_3 bridges three copper ions, the first through a short bond [1.957(3) Å, belonging to the O—N—O chelation], the second to the metal in the position (1/4 − y, x − 3/4,1/4 − z) by a slightly longer bond (1.991 Å), and the third at (1 − x, −1/2 − y, z) through a much longer contact (2.612(3)Å). The methoxy oxygen O_2 is also bonded to the second copper ion generating a five-membered chelation ring involving O_2 and O_3, slightly distorted in an envelope conformation with the metal at the flap deviating 0.45 Å form the plane defined by the chelated system. The copper ion shows a distorted square pyramidal coordination with a longer contact completing a potential octahedron. The

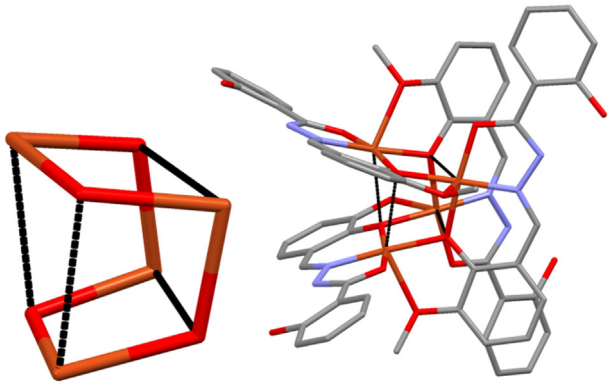

Fig. 5. Left: Cu_4O_4 molecular core of the complex **$Cu_4L_4 \cdot 4CH_3CN$**. The elongation of the dotted bonds is due to the repulsion between ligand evidenced in the image on the right.

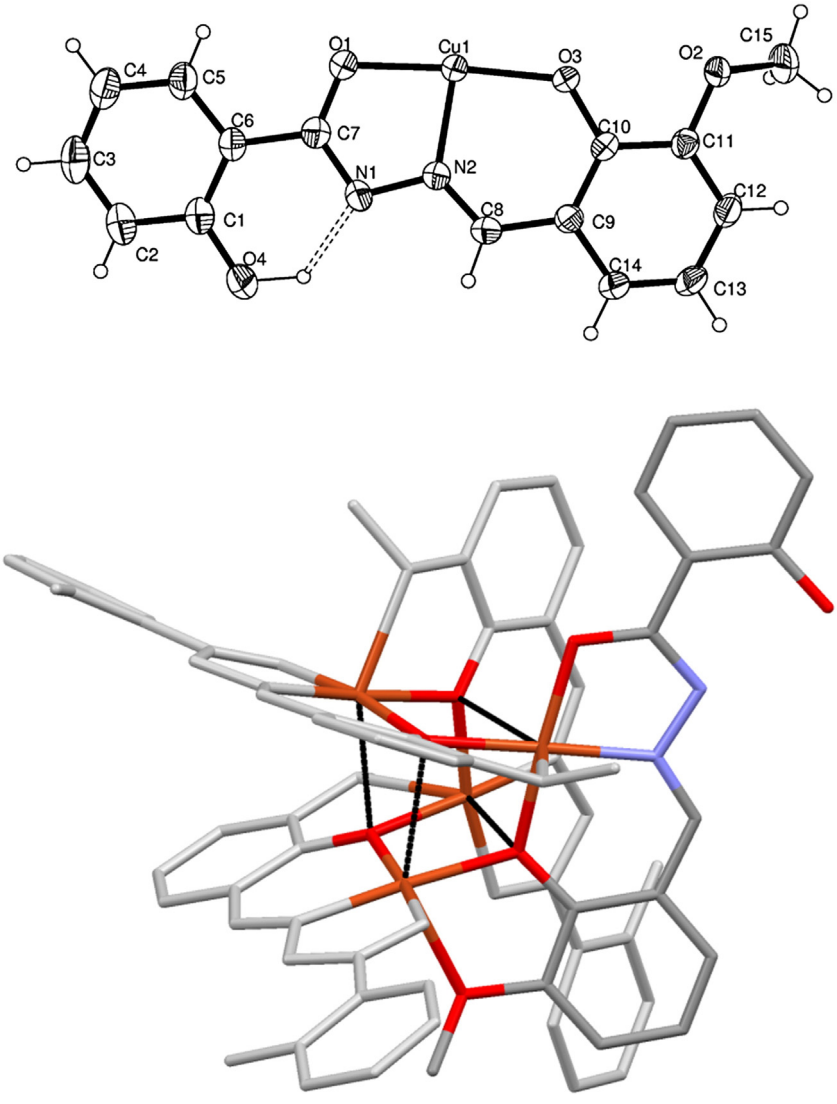

Fig. 4. Molecular structure and labeling, with thermal ellipsoids at the 50% probability level, of the monomeric unit in the complex **$Cu_4L_4 \cdot 4CH_3CN$**.

resulting complex shows a Cu_4L_4 core with eight short (1.957 and 1.991 Å) and four long (2.612 Å) Cu—O distances (Fig. 5). The elongation of these contacts, that hinders the completion of the octahedral coordination, is due to the repulsion between the ligand skeletons that face each other and whose average plane diverge towards the outer part of the complex (Fig. 5). The same complex has been previously described as the DMF solvate [49], showing the same arrangement, the same space group, but a different cell and a different crystal packing; the crystal packing of **$Cu_4L_4 \cdot 4CH_3CN$** is shown in Fig. 6.

Compound (**3**) has been obtained as extremely twinned and weakly diffracting crystals, which nevertheless allowed unambiguous determination of the structure of the salt **$[CoL_2](NHEt_3)$**, shown in Fig. 7.

In the octahedral anionic bischelate complex, the two deprotonated ligands are coordinated by the same tridentate O—N—O chelation observed in the copper tetranuclear complex, forming one six-membered and one five-membered chelate ring with bite angles of 95° and 83°, respectively, for both ligands. As above, the structure of the complex unit is stabilized by an intramolecular OH…N hydrogen bond, with the nitrogen atom of the amide group acting as the hydrogen bond acceptor [O5—H…N3 = 2.56(1) Å, 148(1)°; O1—H…N1 = 2.58(1) Å, 145(1)°]. The $NHEt_3^+$ cation forms a hydrogen bond to the methoxy group of one of the two coordinated ligands [N5—H…O4 = 3.19(2) Å, 170(1)°]. Table 1 reports crystal data and structure analysis.

3.3. Potentiometric measurements

Acylhydrazones represent an interesting class of polydentate, chelating agents with a great variety of complexation modes, due to the possible keto-enol tautomerization and the presence of several potential donor sites. These peculiarities make the study of their speciation in solution very attractive, but at the same time quite complicated to unravel; however this information is essential to try to understand their biological activity and mechanism of action [50]. Potentiometric studies to examine the coordinating behavior of H_2L in solution with a variety of divalent metal ions (Mg^{2+}, Mn^{2+}, Zn^{2+}, Ni^{2+}, Cu^{2+}) were carried out in mixed solvent methanol/water = 9/1 v/v, in which the ligand and almost all the complexes are soluble. The ionic strength was adjusted to 0.1 M KCl. H_2L is diprotic with $pK_{a1} = 8.43 \pm 0.01$ and $pK_{a2} = 12.11 \pm 0.01$; the more acidic group is probably the OH of the *o*-vanillin moiety, and pK_{a2} should be attributed to the dissociation of the salicylic OH. The best fit of the experimental titration curves, carried out in the presence of the metal ions, has been obtained by the Hyperquad software with the sets of species shown in Table 2. The proposed models are corroborated by very good statistical parameters and by nice overlapping between experimental and computed titration curves. The sets reported in Table 2 have been chosen following both the criteria of the minimum standard deviation and of chemical soundness.

For Mg^{2+}, Mn^{2+}, Zn^{2+}, and Ni^{2+}, the species found in solution are MLH, ML_2H, ML, and ML_2 (charges are omitted for simplicity). In solid state the complexes ML_2H_2 are isolated for Mg, Ni and Zn, but, simply by changing the reaction conditions, it is also possible to obtain the species with a stoichiometric ratio 1:1 Mg_2L_2 (**1a**). ZnL_2H_2 can be found, but in low quantities and with a high standard deviation, so it was excluded for statistical reasons.

We have tried sets containing other species, in particular bimetallic species such as M_2LH and M_2L and we can definitely exclude them for Zn^{2+}. To obtain a good fit between experimental and computed titration curves, it is necessary to add to the model the oxydrilated species, formed in small quantities in basic environment. For Mg^{2+} and Zn^{2+}, at high pH the hydroxide $Mg(OH)_2$ and $Zn(OH)_2$ (in our notation MH_{-2}) are found, whereas for Mn^{2+} and Ni^{2+}, the dissociation of a water molecule in the coordination sphere of the metal is suggested, giving rise to MLH_{-1} and ML_2H_{-1}. Oxydrilated species can be disregarded at L/M ratio greater than 1 and at pH lower than 10. The behavior of the ligand with Cu^{2+} in solution is different, in fact the only species that we are able to find is CuL; evidently, as also confirmed by the X-ray structure, the copper(II) ion greatly increases the acidity of the amidic hydrogen and induces

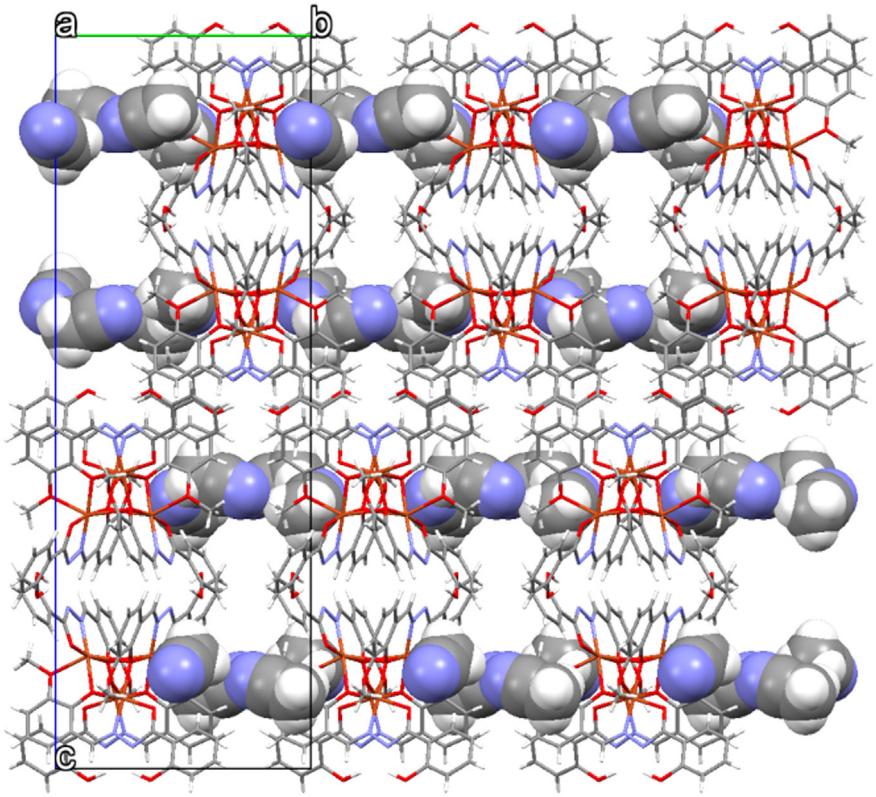

Fig. 6. Crystal packing of **$Cu_4L_4 \cdot 4CH_3CN$** with acetonitrile highlighted in spacefilling representation.

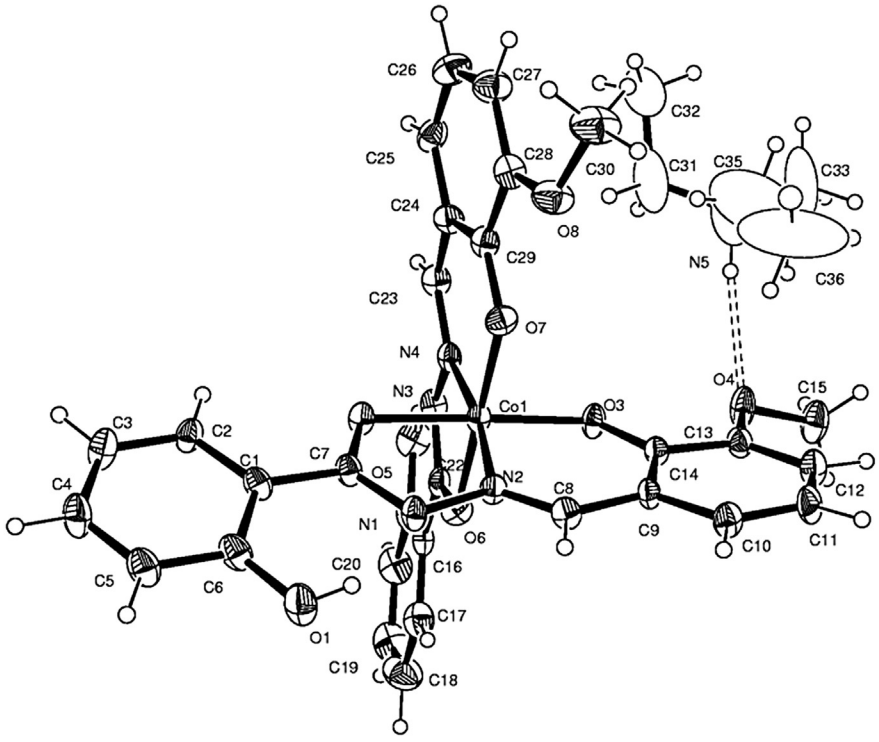

Fig. 7. Crystal structure and labeling of compound (**3**), with thermal ellipsoids at the 50% probability level. The cation has not been shaded for clarity.

bideprotonation of the ligand. It seems therefore that the formation of a tetranuclear cluster is particularly favored by thermodynamic parameters.

Note that we cannot exclude the presence of species with the general formula M_nL_n: the mathematical processing cannot distinguish between the different n values, because the correlation between the species does not allow the convergence of the iterative calculation. Effectively, as already discussed, mass spectrometric data confirm the formation of Cu_4L_4 also in solution, in agreement with the structure of the complex (**5**) isolated in the solid state. The same argument is valid also with the other cations under study: we cannot exclude the formation in solution of dimeric M_2L_2 and/or M_nL_n species, as then effectively isolated at the solid state in (**1a**) (**$Mg_2L_2 \cdot 4H_2O$**) and in (**2**) (**$Mn_2L_2 \cdot 2H_2O$**). The values of the formation constants of the various species differ greatly (Table 2). In particular, as expected, the stability constant for the complexes of Mg^{2+} are the lowest, whereas Ni^{2+} shows the highest affinities. In Fig. 8 the distribution diagrams of the systems formed by the different divalent metal ion and by the ligand under investigation at M/L = 1/2 are compared. It is noteworthy that Mg^{2+} at physiological pH is almost completely present as aqua ion and that the complexation takes place only in basic environment, unlike the other metal ions, for which the complexation already starts at acidic pH.

3.4. Biological activity

As a part of an antiviral testing program conducted in our laboratory [17–20], we evaluated the inhibitory activity of *H_2L* and its metal complexes **1**–**6** against a broad panel of DNA- [i.e., herpes simplex virus type 1 (HSV-1) and type 2 (HSV-2), VV and adenovirus (Ad-2), evaluated in human embryonic lung fibroblast HEL cells] and RNA-viruses (i.e., Coxsackie B4 virus and respiratory syncytium virus, tested in HeLa cells; parainfluenza-3 virus and Punta Toro virus, tested in Vero cells; influenza virus, tested in MDCK cells; human immunodeficiency virus type 1 and type 2, tested in human MT-4 lymphoblast cells; vesicular

Table 2
Logarithms of formation constants ($\beta_{pqr} = [M_pL_qH_r]/[M]^p[L]^q[H]^r$) in methanol/water = 9:1 v/v, I = 0.1 M KCl at 25 °C for the ligand under study with Mg^{2+}, Mn^{2+}, Zn^{2+}, Ni^{2+}, and Cu^{2+}. SDs are given in parentheses.

p	q	r	Mg(II)	Mn(II)	Zn(II)	Ni(II)	Cu(II)
			Log β_{pqr}	Log β_{pqr}	Log β_{pqr}	Log β_{pqr}	Log β_{pqr}
1	1	1	14.87 (0.17)	17.45 (0.05)	17.04 (0.13)	20.58 (0.02)	
1	2	1	22.04 (0.13)	26.23 (0.17)	27.64 (0.14)	32.72 (0.36)	
1	2	0	11.76 (0.07)	17.32 (0.19)	16.28 (0.19)	24.8 (0.59)	
1	1	0	7.64 (0.02)	10.41 (0.04)	10.74 (0.06)	14.51 (0.05)	14.12 (0.01)
1	0	−2	−21.42 (0.09)		−15.52 (0.18)		
1	1	−1		−1.61 (0.05)		3.78 (0.06)	
1	2	−1		5.67 (0.2)		12.62 (0.59)	
0	1	1	L + H = LH	Log β_{011} = 8.43 (0.01)			
0	1	2	L + 2H = LH_2	Log β_{012} = 12.11 (0.01)			

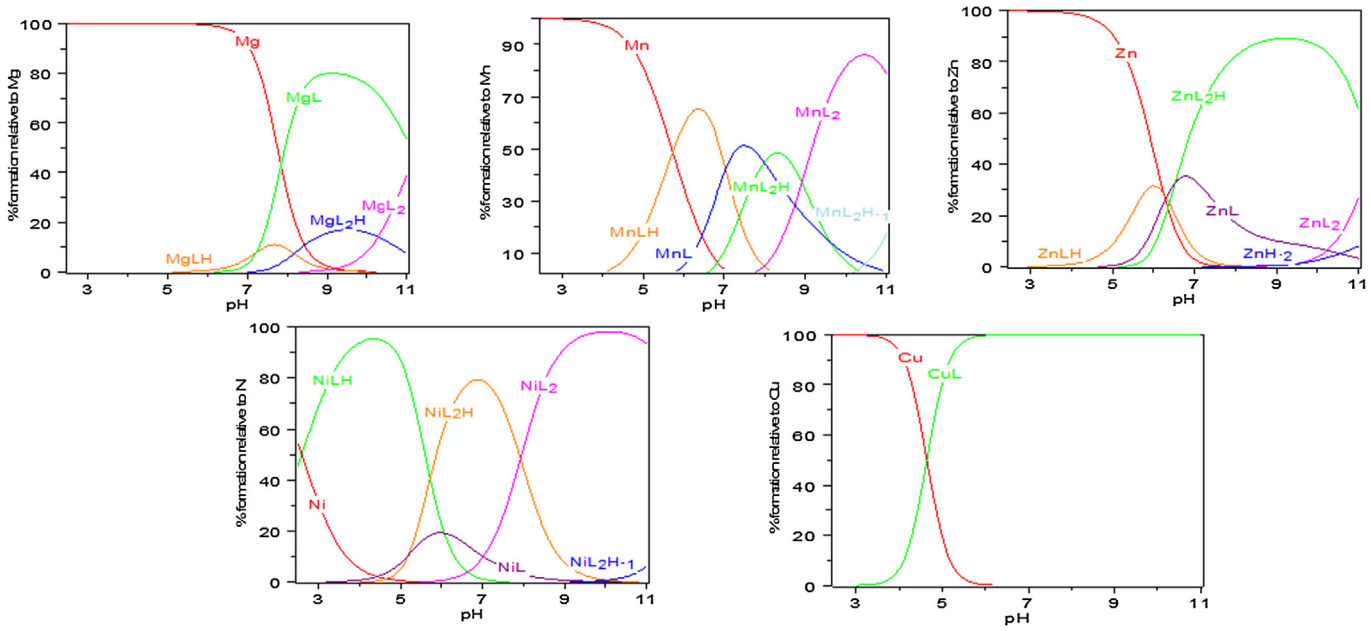

Fig. 8. Distribution diagrams for the systems under investigation at M/L = 1/2 (methanol/water = 9:1 v/v, I = 0.1 M KCl).

stomatitis virus, tested in human embryonic lung fibroblast cells). None of the compounds showed activity against any of the RNA viruses tested, including human immunodeficiency virus type 1 and type 2, and influenza virus (data not shown). For the latter virus, the activities of the compounds were evaluated in a virus yield assay in MDCK cells, as well as in an enzymatic assay with the influenza virus PA endonuclease, which is a Mg^{2+} (or Mn^{2+}) -dependent metalloenzyme [17,20,53].

On the other hand, the tested compounds showed very interesting activity against the DNA-viruses herpes simplex virus (i.e., HSV-1, HSV-2, and an acyclovir-resistant thymidine-kinase deficient HSV-1 strain) and VV. The ligand and metal complexes were not active against Ad-2, which is a naked DNA-virus. To the best of our knowledge, no data are available in the literature about activity of preformed metal complexes with hydrazonic ligands against these viruses.

Table 3
Antiviral activity and cytotoxicity of compounds H_2L and **1**–**6** in cultures of human embryonic lung fibroblast cells.

Compound	Antiviral activity (EC_{50}[a] in μM)						Cytotoxicity MCC[b] in μM
	HSV-1	HSV-1/TK$^-$	HSV-2	VV	VSV	Ad-2	
H_2L	1.6	2.6	2.2	1.3	>100	>100	60
1	1.3	0.8	1.1	0.6	>100	>100	≥20
2	1.1	1.6	0.6	0.5	>100	>100	≥20
3	>100	>100	>100	>100	>100	>100	20
4	1.8	1.8	4.3	2.9	>100	>100	100
5	>100	>100	>100	>100	>100	>100	0.8
6	1.1	0.8	0.8	0.4	>100	>100	≥20
Brivudin	0.05	30	173	17	>250	ND	>250
Acyclovir	0.25	10	0.09	>250	>250	ND	>250
Ganciclovir	0.025	0.5	0.025	>100	>100	ND	>100
Cidofovir	0.95	1.1	0.65	16	>250	7.9	>250
Zalcitabine	ND	ND	ND	ND	ND	7.5	>250
Alovudine	ND	ND	ND	ND	ND	16	>250

Values shown are the average of two independent tests.
ND: not determined.
HSV-1: herpes simplex virus type 1; HSV-1/TK$^-$: acyclovir-resistant thymidine-kinase deficient HSV-1; HSV-2: herpes simplex virus type 2;VV: vaccinia virus; VSV: vesicular stomatitis virus; Ad-2: human adenovirus type 2.
[a] EC_{50}: 50% effective concentration, i.e., compound concentration producing 50% inhibition of virus-induced CPE, determined by microscopy.
[b] MCC: minimum cytotoxic concentration, i.e., compound concentration producing minimal alterations in cell morphology, determined by microscopy.

The antiviral activity and cytotoxicity of H_2L and its complexes **1**–**6** are summarized in Table 3.

It is worth noting that, while (**3**) and (**5**) were inactive, H_2L and its complexes (**1**), (**2**), (**4**) and (**6**) had EC_{50} values in the low micromolar range. Complexes (**1**), (**2**), (**6**) had particularly pronounced activity against VV, with EC_{50} values of 0.6, 0.5 and 0.4 μM, respectively. They had a favorable selectivity index (i.e., ratio of cytotoxic concentration to antivirally effective concentration for VV) in the range of 33–50. One compound in the series, i.e., the copper complex (5) displayed prominent cytotoxicity yet was devoid of antiviral activity.

The biological properties of acylhydrazones and thiosemicarbazones are often related to their coordination abilities [52], or, for example, to the possibility that they may act as carriers for metal ions, allowing penetration of the viral envelope [53].

Clearly, the mechanism of action and precise viral target of the compounds presented here remain to be identified. One possibility worth further investigation is the D10 decapping enzyme of vaccinia virus, which was recently reported to act through a two-metal-ion mechanism [54] and, hence, may be sensitive to metal-chelating inhibitors.

An explanation for the inactivity of the copper and cobalt complexes (**5** and **3**) can be found on structural basis. In fact, the Mg, Mn, Ni and Zn complexes (**1**), (**2**), (**4**) and (**6**) are neutral, with formulas $M(HL)_2$ or Mn_2L_2. On the other hand, (**5**) is a tetranuclear cluster $\mathbf{Cu_4L_4}$ and this cluster is stable also in solution, and (**3**) is the ionic Co(III) complex $\mathbf{[CoL_2](NHEt_3)}$. Therefore, their antiviral inactivity could be related, for example, to insufficient cellular uptake.

Paradoxically, this marked difference in biological activity in relation to a striking structural difference, can be considered as proof that the complexes are stable in the assay conditions.

4. Conclusions

We have started a project focused on the synthesis and biological evaluation of chemical scaffolds that could be able to bind the metal cofactors in the active site of some viral enzymes and, in this way, can inhibit virus replication [17–20,51]. From this perspective, hydrazones seem promising, because of their well-known coordinating abilities and biological properties [4–11,13–16]. We have focused our attention on the *o*-vanillin acylhydrazone scaffold: the potentially tetradentate ligand H_2L shows a great versatility. H_2L promotes the formation of bischelated, tridentate complexes of type $M(HL)_2$ with Mg(II), Ni(II), and

Zn(II), while tetranuclear complexes **Cu_4L_4** are formed with copper divalent ions. The reaction with Co(II), instead, leads to the oxidation of the metal ion and the formation of the bis-chelated ionic complex (**3**), with formula **$[CoL_2](NHEt_3)$**. Versatility in coordination is also a function of pH and, by changing the reaction conditions, it is possible to obtain with Mg(II) the species with a stoichiometric ratio 1:1 Mg_2L_2 (**1a**). Compounds **1**–**6** showed very interesting activity against the DNA-viruses herpes simplex virus (HSV-1; HSV-2; and an acyclovir-resistant thymidine-kinase deficient HSV-1 strain) and VV. In particular, while compounds (**3**) and (**5**) were inactive, the acylhydrazone H_2L and its complexes (**1**), (**2**), (**4**) and (**6**) had EC_{50} values in the low micromolar range. Complexes (**1**), (**2**), (**6**) had particularly pronounced activity against VV, with EC_{50} values of 0.6, 0.5 and 0.4 μM, respectively. The inactivity of (**3**) and (**5**) can be related to their molecular structure, markedly different by that of the bis-chelated, neural complexes (**1**), (**2**), (**4**) and (**6**). Their antiviral inactivity could be related, for example, to insufficient cellular uptake (**3** is ionic; **5** has a high molecular mass). Obviously, the mechanism of action and precise viral target of the compounds presented here remain to be identified, and further investigations will be performed in order to identify the mechanism of action of the *o*-vanillin-benzoylhydrazone scaffold. To the best of our knowledge, no data are present in the literature on antiviral activity of metal complexes of hydrazones ligands on DNA-viruses and this study can help to relate the structural characteristics of the complexes to their antiviral activity.

Abbreviations

VV	vaccinia virus
HSV-1 and HSV-0	herpes simplex virus type 1 and herpes simplex virus type 2
ESI	electrospray ionization
DEP	Direct Exposure Probe
CPE	cytopathic effect
VSV	vesicular stomatitis virus
Ad2	human adenovirus type 2
RSV	respiratory syncytial virus
MDCK cells	Madin–Darby canine kidney cells
HIV-1 and HIV-2	human immunodeficiency virus type 1 and type 2
EC_{50}	50% effective concentration
MCC	minimum cytotoxic concentration

Acknowledgments

The authors acknowledge financial support from the Geconcerteerde Onderzoeksacties-KU Leuven (GOA/15/019/TBA) and the technical assistance from Leentje Persoons and Wim van Dam. D.R., M.C., M.S. thank the Italian Ministero dell'Istruzione, dell'Università e della Ricerca for financial support (PRIN 2010, 2010W2KM5L_003).

Appendix A. Supplementary data

Supplementary data to this article can be found online at http://dx.doi.org/10.1016/j.jinorgbio.2015.05.013.

References

[1] P.H. Lin, T.J. Burchell, R. Clérac, M. Murugesu, Angew. Chem. Int. Ed. Engl. 47 (2008) 8848–8851.
[2] D. Sadhukhan, A. Ray, G. Pilet, C. Rizzoli, G.M. Rosair, C.J. Gómez-García, S. Signorella, S. Bellu, S. Mitra, Inorg. Chem. 50 (2011) 8326–8339.
[3] A. Ray, C. Rizzoli, G. Pilet, C. Desplanches, E. Garibba, E. Rentschler, S. Mitra, Eur. J. Inorg. Chem. (2009) 2915–2928.
[4] T. Nasr, S. Bondock, M. Youns, Eur. J. Med. Chem. 76 (2014) 539–548.
[5] F. Bisceglie, S. Pinelli, R. Alinovi, P. Tarasconi, A. Buschini, F. Mussi, A. Mutti, G. Pelosi, J. Inorg. Biochem. 116 (2012) 195–203.
[6] T.W. Sanchez, B. Debnath, F. Christ, H. Otake, Z. Debyser, N. Neamati, Bioorg. Med. Chem. 21 (2013) 957–963.
[7] A. Herschhorn, C. Gu, N. Espy, J. Richard, A. Finzi, J.G. Sodroski, Nat. Chem. Biol. 10 (2014) 845–852.
[8] M. Sutradhar, M.V. Kirillova, M.F. Guedes da Silva, C.-M. Liu, A.J.L. Pombeiro, Dalton Trans. 42 (2013) 16578–16587.
[9] H.H. Monfared, Z. Kalantari, M.-A. Kamyabi, C. Janiak, Z. Anorg. Allg. Chem. 633 (2007) 1945–1948.
[10] M. Albrecht, Y. Liu, S.S. Zhu, C.A. Schalley, R. Fröhlich, Chem. Commun. (2009) 1195–1197.
[11] G.M. Yu, L. Zhao, Y.N. Guo, G.F. Xu, L.F. Zou, J. Tang, Y.H. Li, J. Mol. Struct. 982 (2010) 139–144.
[12] O. Pouralimardan, A.C. Chamayou, C. Janiak, H. Hosseini-Monfared, Inorg. Chim. Acta 360 (2007) 1599–1608.
[13] V.J. Negi, A.K. Sharma, J.S. Negi, V. Ram, Int. J. Pharm. Chem. 2 (2012) 100–109.
[14] G. Verma, A. Marella, M. Shaquiquzzaman, M. Akhtar, M.R. Ali, M.M. Alam, J. Pharm. Bioallied Sci. 6 (2014) 69–80.
[15] M.M.E. Shakdofa, M.H. Shtaiwi, N. Morsy, T.M.A. Abdel-rassel, Main Group Chem. 13 (2014) 187–218.
[16] S. Rollas, S.G. Küçükgüzel, Molecules 12 (2007) 1910–1939.
[17] M. Carcelli, D. Rogolino, A. Bacchi, G. Rispoli, E. Fisicaro, C. Compari, M. Sechi, A. Stevaert, L. Naesens, Mol. Pharm. 11 (2014) 304–316.
[18] D. Rogolino, M. Carcelli, C. Compari, L. De Luca, S. Ferro, E. Fisicaro, G. Rispoli, N. Neamati, Z. Debyser, F. Christ, A. Chimirri, Eur. J. Med. Chem. 78 (2014) 425–430.
[19] M. Carcelli, D. Rogolino, M. Sechi, G. Rispoli, E. Fisicaro, C. Compari, N. Grandi, A. Corona, E. Tramontano, C. Pannecouque, L. Naesens, Eur. J. Med. Chem. 83 (2014) 594–600.
[20] A. Stevaert, S. Nurra, N. Pala, M. Carcelli, D. Rogolino, C. Shepard, R.A. Domaoal, B. Kim, M. Alfonso-Prieto, S.A.E. Marras, M. Sechi, L. Naesens, Mol. Pharmacol. 87 (2015) 323–337.
[21] D. Rogolino, M. Carcelli, M. Sechi, N. Neamati, Coord. Chem. Rev. 256 (2012) 3063–3086.
[22] K.A. Kirby, B. Marchand, Y.T. Ong, T.P. Ndongwe, A. Hachiya, E. Michailidis, M.D. Leslie, D.V. Sietsema, T.L. Fetterly, C.A. Dorst, K. Singh, Z. Wang, M.A. Parniak, S.G. Sarafianos, Antimicrob. Agents Chemother. 56 (2012) 2048–2061.
[23] L.Z. Sacconi, Z. Anorg. Allg. Chem. 275 (1954) 249–256.
[24] E. Fisicaro, A. Braibanti, Talanta 35 (1988) 769–774.
[25] G. Gran, Analyst 77 (1952) 661–671.
[26] P. Gans, A. Sabatini, A. Vacca, Talanta 43 (1996) 1739–1753.
[27] O.V. Dolomanov, L.J. Bourhis, R.J. Gildea, J.A.K. Howard, H. Puschmann, J. Appl. Crystallogr. 42 (2009) 339–341.
[28] M.C. Burla, R. Caliandro, M. Camalli, B. Carrozzini, G.L. Cascarano, L. De Caro, C. Giacovazzo, G. Polidori, D. Siliqi, R. Spagna, J. Appl. Crystallogr. 40 (2007) 609–613.
[29] G.M. Sheldrick, Acta Crystallogr. A. 64 (2008) 112–122.
[30] M. Nardelli, J. Appl. Crystallogr. 28 (1995) 659.
[31] F.H. Allen, O. Kennard, R. Taylor, Acc. Chem. Res. 16 (1983) 146–153.
[32] I.J. Bruno, J.C. Cole, P.R. Edgington, M. Kessler, C.F. Macrae, P. McCabe, J. Pearson, R. Taylor, Acta Crystallogr. B 58 (2002) 389–397.
[33] G. Palla, G. Predieri, P. Domiano, C. Vignali, W. Turner, Tetrahedron 42 (1986) 3649–3654.
[34] B.D. Wang, Z.Y. Yang, Q. Wang, T.K. Cai, P. Crewdson, Bioorg. Med. Chem. 14 (2006) 1880–1888.
[35] Y.H. Li, Z.Y. Yang, B.D. Wang, Transition Met. Chem. 31 (2006) 598–602.
[36] Q. Wang, Y. Wang, Z.Y. Yang, Chem. Pharm. Bull. 56 (2008) 1018–1021.
[37] S. Zhao, L. Li, X. Liu, W. Feng, X. Lü, Acta Crystallogr., Sect. E Struct. Rep. Online 68 (2012) o2040.
[38] J.T. Lei, Y.X. Jiang, L.Y. Tao, S.S. Huang, H.L. Zhang, Acta Crystallogr., Sect. E Struct. Rep. Online 64 (2008) o909.
[39] S.Q. Wu, Y.T. Wang, A.L. Cui, H.Z. Kou, Inorg. Chem. 53 (2014) 2613–2618.
[40] A.R. Stefankiewicz, G. Rogez, J. Harrowfield, M. Drillon, J.M. Lehn, Dalton Trans. (2009) 5787–5802.
[41] Z.A. Siddiqi, A. Siddique, M. Shahid, M. Khalid, P.K. Sharma, M. Ahmad Anjuli, S. Kumar, Y. Lan, A.K. Powell, Dalton Trans. 42 (2013) 9513–9522.
[42] H.H. Monfared, J. Sanchiz, Z. Kalantari, C. Janiak, Inorg. Chim. Acta 362 (2009) 3791–3795.
[43] M. Sutradhar, G. Mukherjee, M.G.B. Drew, S. Ghosh, Inorg. Chem. 45 (2006) 5150–5161.
[44] R. Dinda, P. Sengupta, M. Sutradhar, T.C.W. Mak, S. Ghosh, Inorg. Chem. 47 (2008) 5634–5640.
[45] M. Sutradhar, T. Roy Barman, G. Mukherjee, M.G.B. Drew, S. Ghosh, Polyhedron 34 (2012) 92–101.
[46] M. Sutradhar, T. Roy Barman, S. Ghosh, M.G.B. Drew, J. Mol. Struct. 1020 (2012) 148–152.
[47] M.N. Kopylovich, A.C.C. Nunes, K.T. Mahmudov, M. Haukka, T.C.O. Mac Leod, L.M.D.R.S. Martins, M.L. Kuznetsov, A.J.L. Pombeiro, Dalton Trans. 40 (2011) 2822–2836.
[48] H. Hosseini-Monfared, R. Bikas, P. Mahboubi-Anarjan, A.J. Blake, V. Lippolis, N.B. Arslan, C. Kazak, Polyhedron 69 (2014) 90–102.
[49] M.L. Liu, J.M. Dou, J.Z. Cui, D.C. Li, D.Q. Wang, J. Mol. Struct. 1011 (2012) 140–144.
[50] S. Hakobyan, J.-F. Boily, M. Ramstedt, J. Inorg. Biochem. 138 (2014) 9–15.
[51] A. Stevaert, R. Dallocchio, R. Dessì, N. Pala, D. Rogolino, M. Sechi, L. Naesens, J. Virol. 87 (2013) 10524–10538.
[52] I.J. Kang, L.W. Wanga, T.A. Hsu, A. Yueh, C.C. Lee, Y.C. Lee, C.Y. Lee, Y.S. Chao, S.R. Shih, J.H. Chern, Bioorg. Med. Chem. Lett. 21 (2011) 1948–1952.
[53] G. Pelosi, F. Bisceglie, F. Bignami, P. Ronzi, P. Schiavone, M.C. Re, C. Casoli, E. Pilotti, J. Med. Chem. 53 (2010) 8765–8769.
[54] M.F. Soulière, J.P. Perreault, M. Bisaillon, Biochem. J. 420 (2009) 27–35.